

Approaching the Glass Transition Temperature of GeTe by Crystallizing Ge₁₅Te₈₅

Julian Pries, Yuan Yu, Peter Kerres, Maria Häser, Simon Steinberg, Fabian Gladisch, Shuai Wei, Pierre Lucas, and Matthias Wuttig*

Like many phase-change materials, GeTe crystallizes upon heating at a conventional rate before the calorimetric glass transition is reached. This has so far prevented an unambiguous determination of its glass transition temperature T_g . Herein, a new approach is realized to estimate the glass transition temperature T_g for GeTe through progressive crystallization of Ge₁₅Te₈₅. Selective crystallization of pure tellurium during sub- T_g annealing leads to a gradual change in the composition of the amorphous surrounding toward that of GeTe. This gives rise to a new endotherm whose onset temperature gradually approaches the T_g of GeTe.

bonding (MVB).^[4–6] To improve data transfer rates, a comprehensive understanding of crystallization kinetics is crucial.^[7] Specifying the viscosity's temperature dependence is of major interest for this purpose since the nucleation rate I and crystal growth velocity v_g are inversely proportional to viscosity η .^[8–12] To describe the viscosity as a function of temperature of the liquid and undercooled liquid phase (UCL),^[13] the fragility m ^[14] and the glass transition temperature T_g of the material are essential. The fragility can be given by^[14,15]

$$m = \left. \frac{d \log_{10} \eta}{dT_g/T} \right|_{T=T_g} \quad (1)$$

Phase-change materials (PCMs) such as GeTe or Sb₂Te₃ are a class of materials that can be switched rapidly between two solid phases.^[1,2] These two solid phases, namely the amorphous and crystalline phase, feature a contrast in optical and electrical properties that makes them suitable for optical and electrical data storage devices.^[2] This property contrast was previously explained by a change in chemical bonding: while the amorphous phase is covalently bonded,^[3] the crystalline phase shows metavalent

Unfortunately, values of T_g for GeTe reported in literature vary from as low as 150 °C up to 230 °C.^[16–21] This large variation results in a large and unfavorable uncertainty when it comes to predicting crystallization kinetics for PCM-based data storage devices. For this reason, an accurate value based on experimental data for the glass transition temperature T_g of GeTe is highly desirable.

An attempt at measuring the glass transition temperature of amorphous GeTe is shown in **Figure 1**. Here, amorphous powder prepared by magnetron sputter deposition was heated in a Differential scanning calorimeter (DSC) at a constant heating rate of 40 K min^{−1} after annealing at increasing temperatures for 1 h. As **Figure 1** shows, the DSC trace of the unannealed (as-deposited) GeTe exhibits a broad exotherm starting at around 95 °C, before crystallization is initiated at 165 °C. Upon annealing up to 115 °C, the crystallization remains largely unaffected, whereas the exotherm before crystallization progressively disappears. This is a well-established consequence of enthalpy release from the glassy phase due to structural relaxation in hyperquenched glasses and it has been observed in other PCMs like Ge₂Sb₂Te₅,^[22,23] chalcogenide,^[22,24] oxide,^[25,26] metallic glasses,^[27] and other glasses before. However, instead of showing a glass transition endotherm following the relaxation exotherm, crystallization sets in. Thus, obscuring any thermal event that could have signaled a glass transition. Therefore, it becomes clear that the glass transition temperature of amorphous GeTe cannot be directly measured from heating due to fast crystallization.


A similar enthalpy relaxation phenomenon is shown in **Figure 2a,b** for Ge₁₅Te₈₅. As for GeTe, the enthalpy release caused by structural relaxation of the glassy phase is largely

J. Pries, Dr. Y. Yu, P. Kerres, M. Häser, Prof. M. Wuttig
Institute of Physics IA
RWTH Aachen University
52074 Aachen, Germany
E-mail: wuttig@physik.rwth-aachen.de

Dr. S. Steinberg, F. Gladisch
Institute of Chemistry
RWTH Aachen University
52074 Aachen, Germany

Prof. S. Wei
Department of Chemistry
Aarhus University
DK-8000 Aarhus-C, Denmark

Prof. P. Lucas
Department of Materials Science and Engineering
University of Arizona
Tucson, AZ 85721, USA

 The ORCID identification number(s) for the author(s) of this article can be found under <https://doi.org/10.1002/pssr.202000478>.

© 2020 The Authors. Physica Status Solidi (RRL) - Rapid Research Letters published by Wiley-VCH GmbH. This is an open access article under the terms of the Creative Commons Attribution-NonCommercial License, which permits use, distribution and reproduction in any medium, provided the original work is properly cited and is not used for commercial purposes.

DOI: 10.1002/pssr.202000478

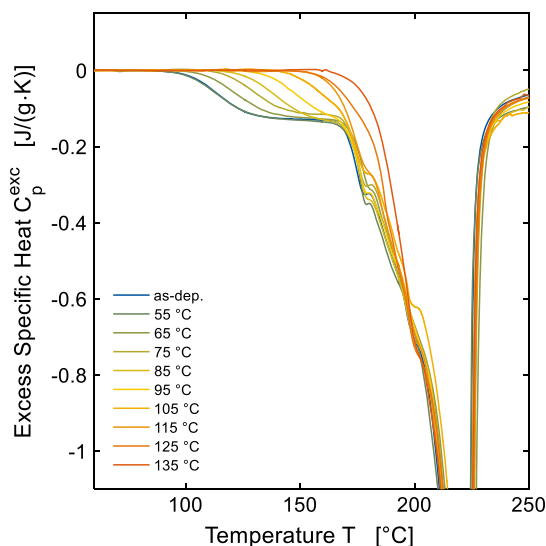


Figure 1. Excess heat capacity C_p^{exc} of amorphous GeTe powder obtained by DSC after an annealing at the indicated temperature for 1 h followed by heating with a rate $\dot{\theta}_h$ of 40 K min⁻¹. Upon heating amorphous GeTe starts releasing heat due to structural relaxation beginning at 95 °C for the as-deposited state. Crystallization is initiated at about 165 °C for all heat treatments depicted and shows its maximum at 223 °C. There are two shoulders in the crystallization exotherm: one at 180 °C and the other at around 200 °C. While the exothermic heat release before crystallization indicates structural relaxation of the glassy amorphous state, the glass transition is not observed before crystallization starts.

influenced by annealing. This is expected as long as the annealing temperature is below the glass transition temperature of the material (or to be precise, its fictive temperature T_f).^[28] Differing

from that in GeTe, in Ge₁₅Te₈₅ the exothermic heat release is followed by a glass transition without crystallization interfering. The glass transition temperature T_g can be measured from the onset of the glass transition to be 135 °C for the unannealed (as-deposited) material, see Figure 2, which is close to the T_g of the melt-quenched glass of the same composition.^[24,29] Following the glass transition, the material enters and remains in the UCL up to the onset of crystallization at around 185 °C. Interestingly, there are two exothermic crystallization events peaking at 220 and 230 °C.

As the annealing temperature increases, the enthalpy trapped during quenching is progressively released and the relaxation exotherm develops into an endothermic overshoot. When the annealing temperature becomes larger than T_g , the material enters the UCL during annealing and since the UCL is a (meta-)stable equilibrium phase, annealing does not lead to any further enthalpy decrease.^[28] When cooled again at a constant cooling rate of 40 K min⁻¹, the UCL vitrifies and the resulting glasses feature the same enthalpy state. Therefore, the excess heat capacity C_p^{exc} curves after annealing at 135–150 °C in Figure 2 are almost identical. During annealing at higher temperatures in the range of 155–180 °C, partial crystallization occurs as shown in the X-ray diffraction (XRD) patterns shown in Figure 3, leading to a continuous decrease in the glass transition endotherm of Ge₁₅Te₈₅ at 140 °C, see Figure 4a. Simultaneously, the C_p^{exc} value in the temperature range of 150–180 °C decreases, whereas its slope increases showing signs of an emerging endotherm at higher temperatures that becomes most prominent at annealing temperatures of 180–190 °C. This emerging endotherm cannot be explained only by a decrease in Ge₁₅Te₈₅ content. Meanwhile, during annealing at 155–180 °C, the first crystallization peak decays until it eventually vanishes

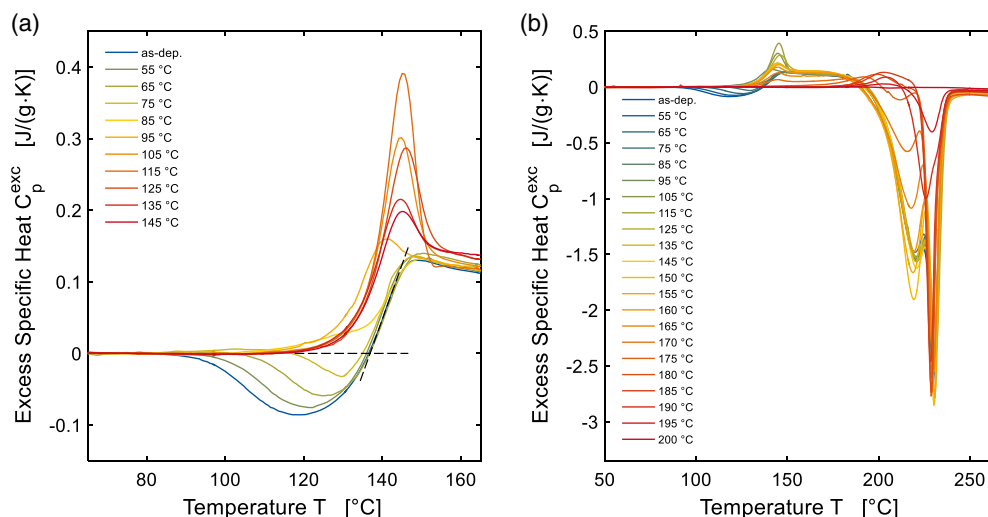


Figure 2. Excess heat capacity C_p^{exc} of amorphous Ge₁₅Te₈₅ powder obtained by DSC after an annealing at the indicated temperature for 1 h and subsequent heating with a rate $\dot{\theta}_h$ of 40 K min⁻¹. Similar to Figure 1, in (a) the exothermic heat release due to structural relaxation of the glassy phase is visible starting at 90 °C for the as-deposited phase. The enthalpy relaxation exotherm is followed by the glass transition with a glass transition temperature T_g of 135 °C (as-dep.). The onset construction to obtain the glass transition temperature is depicted by the dashed lines. The undercooled liquid (UCL) is observed in between the glass transition and the onset of crystallization at about 185 °C, see (b). Note that crystallization consists of two individual processes indicated by the two distinct peaks with peak temperatures of 220 and 230 °C. In addition to the changes to the glass transition induced by annealing, the first crystallization peak can be removed completely by annealing at 185 °C for 1 h, whereas the second peak remains unaffected. At this annealing temperature, an unexpected endotherm is observed around 200 °C, see (b).

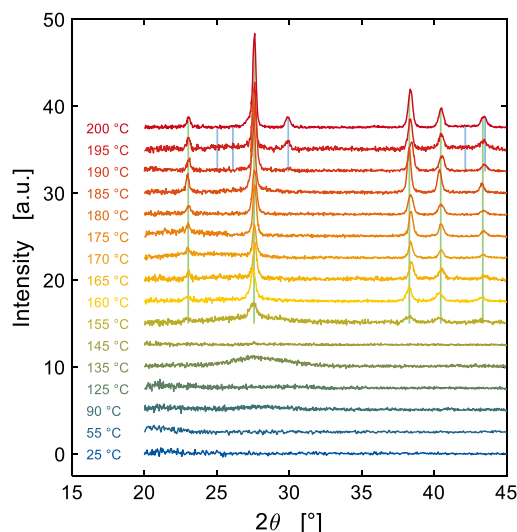


Figure 3. XRD of $\text{Ge}_{15}\text{Te}_{85}$ powder after annealing at the indicated temperature for 1 h. The powder for XRD and DSC measurements on $\text{Ge}_{15}\text{Te}_{85}$ was obtained from the same preparation process. The XRD scans show that crystallization is first initiated during the 1 h annealing at 155 °C. All peaks appearing up to an annealing temperature of 185 °C can be attributed to crystalline tellurium (light green vertical lines).^[32] These peaks become more pronounced for each annealing step up to 185 °C. The first GeTe diffraction peak that appears is the (102) peak at 29.9°^[33] at an annealing temperature of 190 °C. It grows in intensity with increasing annealing temperature (see light blue vertical lines for GeTe reflections). A close-up around this peak is shown in the Supporting Information.

completely at 185 °C, whereas the second peak remains largely the same, see Figure 2b. At an annealing temperature of 190 °C the second peak also decreases until it vanishes at 200 °C, too. Interestingly, the more the first crystallization peak is reduced by annealing, the more prominent the second endotherm near 200 °C becomes.

The multiple thermal events shown in Figure 2a,b can be understood by considering that $\text{Ge}_{15}\text{Te}_{85}$ is a eutectic composition.^[30] Once crystallized, it consists of 70% crystalline tellurium and 30% crystalline GeTe. Hence, the two crystallization events in Figure 2 could be related to the crystallization of these two crystalline phases. Support for this hypothesis is found in the study by Sengottaiyan et al.^[31] and others, where tellurium was found to crystallize first. This is confirmed by the XRD data shown in Figure 3. Here, as in the DSC-measurements from Figure 2, first signs for crystallization are found for an annealing temperature of 155 °C when the first diffraction peaks start to appear. This is also the annealing temperature where the glass transition endotherm of $\text{Ge}_{15}\text{Te}_{85}$ starts to decrease, see Figure 2 and 4a. All diffraction peaks are attributed to crystalline tellurium (space group: 152^[32]) up to an annealing of 185 °C, which confirms that tellurium crystallizes first. This is in line with changes in the excess heat capacity C_p^{exc} curves, where only the first crystallization peak is affected by annealing as an increasing fraction of tellurium is crystallized during annealing. Finally, at an annealing temperature of 190 °C or higher, diffraction peaks for GeTe (space group: 160^[33]) appear and increase up to an annealing temperature of 200 °C. For a close-up around the most prominent GeTe reflection, see Figure S1, Supporting Information. Simultaneously, the second crystallization peak in

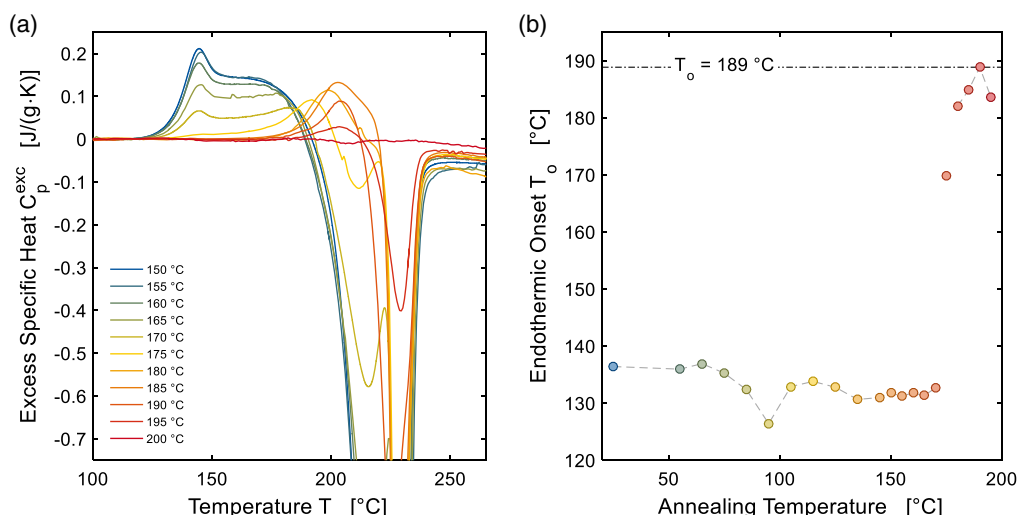


Figure 4. a) Close-up of excess heat capacity curves for the highest annealing temperatures from Figure 2. When the annealing temperature is increased from 155 to 185 °C, the first crystallization peak disappears and instead an endotherm develops. This first crystallization peak has been attributed to the formation of crystalline tellurium from XRD data, whereas the second peak is assigned to GeTe crystallization. The corresponding DSC peak is influenced notably only at an annealing of 190 °C or higher and the crystallization peak disappears at an annealing at 200 °C. After annealing at 200 °C for 1 h, the sample has completed crystallization. b) Endothermic onset temperature after annealing at the indicated temperatures for 1 h. At low annealing temperatures, this onset is the glass transition of as-deposited $\text{Ge}_{15}\text{Te}_{85}$. It is decreasing up to an annealing of 95 °C when the shadow glass transition and glass transition merge and subsequently jumps up at 105 °C. The onset temperature experiences a rapid jump when the annealing temperature increases from 170 to 175 °C. When the tellurium has crystallized (at $T_{\text{an}} = 185$ °C, see Figure 3 and 4a) the endotherm can only be caused by the glass transition of the remaining amorphous material which is approaching the composition of GeTe. Therefore, the measured onset temperature of 189 °C provides an estimate for the glass transition temperature T_g of GeTe.

C_p^{exc} curves decreases and vanishes at 200 °C. For more details, see Figure S2, Supporting Information. By combining the findings from XRD and DSC, the first crystallization peak can be attributed to the crystallization of tellurium, whereas the second crystallization peak is attributed to the crystallization of GeTe.

DSC and XRD data demonstrate that crystallization in $\text{Ge}_{15}\text{Te}_{85}$ takes place in two distinct processes where the crystallization of tellurium is followed by that of GeTe. By proper annealing, a volume fraction x of tellurium can be crystallized without crystallizing GeTe, see Figure 3. This volume fraction is thus removed from the remaining amorphous material leading to a composition change according to $\text{Ge}_{15}\text{Te}_{(85-x)}$ by the

diffusion of germanium into the amorphous phase and tellurium into the crystal. This means that the composition of the amorphous material changes towards GeTe, as shown in Figure 5.

As soon as the composition starts changing, an unexpected endotherm near 200 °C develops which must be caused by the glass transition of the remaining (glassy) amorphous material that was formed upon cooling the UCL after annealing, whose presence is shown in Figure S3, Supporting Information. Hence, from the onset temperature of this endotherm, the glass transition temperature T_g of the remaining amorphous material can be deduced, see Figure 4b. Upon the crystallization of tellurium, the high-temperature endotherm and its onset shift to

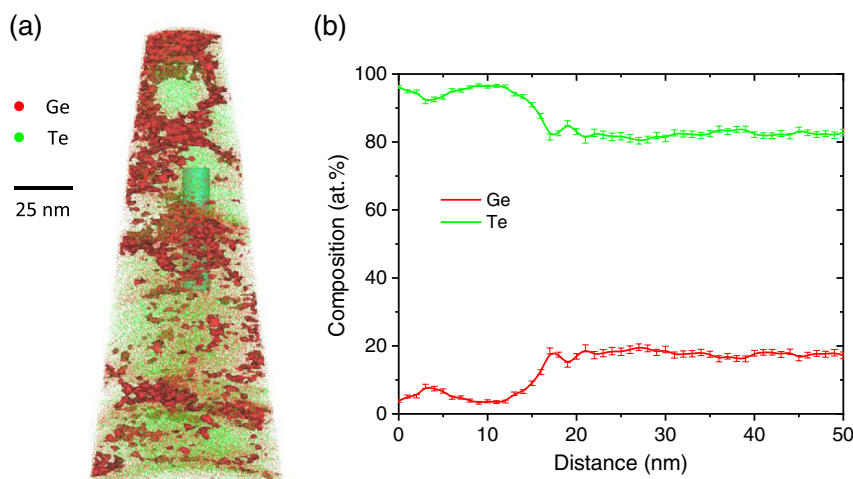


Figure 5. APT of locally detected ions of a $\text{Ge}_{15}\text{Te}_{85}$ sample annealed at 170 °C for 1 h. The powder for APT, XRD, and DSC measurements of $\text{Ge}_{15}\text{Te}_{85}$ was obtained in the same preparation process. a) Tellurium is shown in green and germanium in red. Regions of crystallized tellurium are clearly visible. Regions containing more than 20% of germanium are enclosed by a red isosurface. The concentration profile within the turquoise cylinder is shown in (b). The germanium content of the remaining amorphous phase outside the tellurium crystal shows a constant base level of about 20% after a transition region of about 5 nm.

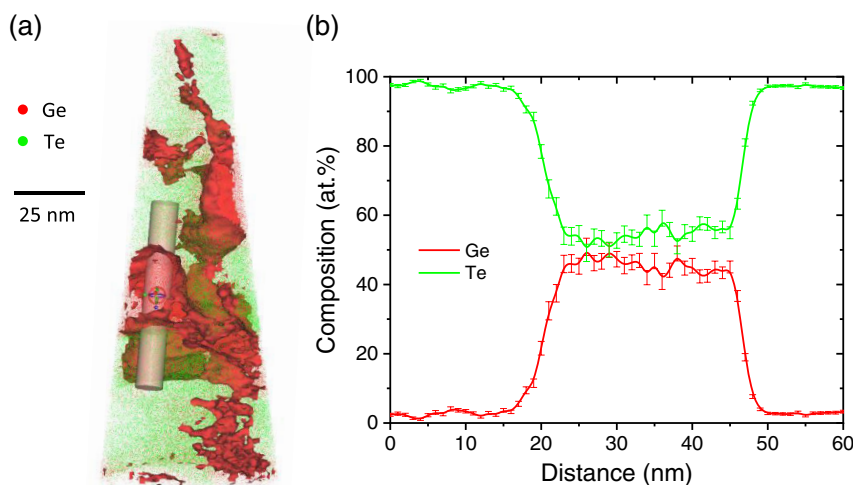


Figure 6. APT of locally detected ions of a $\text{Ge}_{15}\text{Te}_{85}$ sample annealed at 200 °C for 1 h. The powder for APT, XRD, and DSC measurements of $\text{Ge}_{15}\text{Te}_{85}$ was obtained in the same preparation process. a) The local distribution of tellurium (green) and germanium (red) is shown. Regions of crystallized tellurium and GeTe are clearly distinguishable. Regions containing more than 30% of germanium are enclosed by a red isosurface. The concentration profile within the cylinder in (a) is shown in (b). The germanium concentration outside the tellurium crystals has reached the final concentration of GeTe within experimental uncertainty (error bars in (b) indicate the standard deviation of the various composition values determined in the selected area).

higher temperatures, as shown in Figure 4a,b, as the composition of the remaining amorphous phase $\text{Ge}_{15}\text{Te}_{(85-x)}$ shifts toward the composition of GeTe, see Figure 6. Therefore, the glass transition temperature of the PCM GeTe is then defined as the maximum onset of the high-temperature endotherm at $\approx 190^\circ\text{C}$, as shown in Figure 4b. It is discussed in the Supporting Information, if the composition of $\text{Ge}_{50}\text{Te}_{50}$ can finally be reached and how robust the observed glass transition temperature is to a change in composition.

While the glass transition of pure GeTe is obscured by crystallization, see Figure 1, the glass transition of GeTe becomes observable in annealed $\text{Ge}_{15}\text{Te}_{85}$, see Figure 2 and 4a, as here the onset of crystallization of GeTe is postponed by $\approx 40^\circ\text{C}$, whereas the crystallization peak temperature is postponed by 10°C . There could be two reasons for this delay. On the one hand, as shown in Figure 6, the size of the GeTe containing areas is within the tens of nanometers range. This size might be small enough for confinement effects to become important. On the other hand, the crystallization of GeTe in annealed $\text{Ge}_{15}\text{Te}_{85}$ is made possible by the diffusion processes involved due to tellurium crystallization. Therefore, it may take some time until the Ge content becomes high enough for GeTe to initialize crystallization.

In this study, we have shown at first that a direct measurement of the calorimetric glass transition of pure GeTe fails because the glass transition is obscured by crystallization (Figure 1), just as it was found previously in another MVB showing material ($\text{Ge}_2\text{Sb}_2\text{Te}_5$).^[22] Therefore, we have explored an alternative route. We studied $\text{Ge}_{15}\text{Te}_{85}$, a eutectic composition that transforms during crystallization into tellurium and GeTe where the tellurium crystallizes first and GeTe crystallizes afterward. Increasing the annealing temperature leads to tellurium crystallization, which in turn shifts the local and average composition of the remaining amorphous material from the initial $\text{Ge}_{15}\text{Te}_{85}$ toward that of GeTe (also see Supporting Information). As the remaining amorphous material approaches the composition of GeTe, a high-temperature endotherm develops which is identified to be the glass transition of this material. This endotherm serves as the basis for approximating the glass transition temperature T_g for GeTe to be around 190°C .

Experimental Section

Powders for DSC, XRD, TEM and atom probe tomography (APT) measurements of $\text{Ge}_{15}\text{Te}_{85}$ and GeTe were prepared from stoichiometric targets by magnetron sputter deposition at a base pressure of 3×10^{-6} mbar. The composition was confirmed via scanning electron microscopy (SEM) in a FEI Helios Dual Beam FIB. The excess heat capacity C_p^{exc} was obtained in a Perkin Elmer Diamond DSC by subtracting the crystalline rescan from the initial scan. The melting onset of pure indium was used to calibrate the temperature at a constant heating $\dot{\theta}$ as already reported in the Supporting Information in the study by Pries et al.^[22]

The XRD data were measured with a Bruker D8 Discover diffractometer in a reflection setup. The powder was placed on a single crystal silicon substrate and illuminated with parallel $\text{Cu K}\alpha 1$ radiation at a fixed glancing angle of 1° . The 2θ scans were obtained with a 1D LynxEye Silicon strip detector. For better comparability, the diffuse scattering background of the XRD scans was removed in Figure 3.

The needle-shaped APT specimen were prepared by a cross-beam focused ion beam (FIB, Helios NanoLab 650, FEI) according to the standard “lift-out” method. Low voltage (2 kV) was applied to the final

APT specimen to remove any Ga contaminations due to the preparation process. APT characterization was carried out using a local electrode APT (LEAP 4000X Si, CAMECA) with an ultraviolet laser ($\lambda = 355$ nm, repetition rate of 200 kHz). The laser pulse energy was 5 pJ, the base temperature of the specimen was 40 K, the average detection rate was 1% and the flight path of ions was 160 mm. Data reconstruction and analyses were processed using IVAS 3.8.0.

Supporting Information

Supporting Information is available from the Wiley Online Library or from the author.

Acknowledgements

The authors acknowledge funding from the Deutsche Forschungsgemeinschaft (DFG) via the collaborative research center Nanoswitches (SFB 917) and in part by the Federal Ministry of Education and Research (BMBF, Germany) in the project NEUROTEC (16ES1133 K). P.L. acknowledges funding from NSF-DMR grant No. 1832817. S.W. acknowledges the support of the DFG grant No. 422219280. S.S. acknowledges funding from Fonds der Chemischen Industrie. Support with XRD measurements by Tobias Strop is gratefully appreciated as well as the supervision of the APT setup by Oana Cojocaru-Mirédin and by Svitlana Taranenko. Jean-Marc Joubert is gratefully acknowledged for conducting and providing us with the CALPHAD calculations of the stable and metastable phase diagrams and all helpful discussions and comments. The authors thank the anonymous reviewers for critically reading the manuscript and suggesting improvements concerning the stoichiometry of the glassy phase, whose T_g is determined in this work. Open access funding enabled and organized by Projekt DEAL.

Conflict of Interest

The authors declare no conflict of interest.

Keywords

crystallization kinetics, glass transition, metavalent bonding, phase-change materials, undercooled liquids

Received: October 2, 2020

Revised: November 6, 2020

Published online: November 24, 2020

- [1] M. Wuttig, N. Yamada, *Nat. Mater.* **2007**, 6, 824.
- [2] D. Lencer, M. Salinga, B. Grabowski, T. Hickel, J. Neugebauer, M. Wuttig, *Nat. Mater.* **2008**, 7, 972.
- [3] M. Zhu, O. Cojocaru-Mirédin, A. M. Mio, J. Keutgen, M. Küpers, Y. Yu, J.-Y. Cho, R. Dronskowski, M. Wuttig, *Adv. Mater.* **2018**, 30, 1706735.
- [4] J. Y. Raty, M. Schumacher, P. Golub, V. L. Deringer, C. Gatti, M. Wuttig, *Adv. Mater.* **2019**, 31, 1806280.
- [5] M. Wuttig, V. L. Deringer, X. Gonze, C. Bichara, J. Y. Raty, *Adv. Mater.* **2018**, 30, 1803777.
- [6] B. J. Kooi, M. Wuttig, *Adv. Mater.* **2020**, 32, 1908302.
- [7] J. Pries, O. Cojocaru-Mirédin, M. Wuttig, *MRS Bull.* **2019**, 44, 699.
- [8] A. Sebastian, M. Le Gallo, D. Krebs, *Nat. Commun.* **2014**, 5, 4314.
- [9] M. Salinga, E. Carria, A. Kalenbach, M. Bornhöft, J. Benke, J. Mayer, M. Wuttig, *Nat. Commun.* **2013**, 4, 2371.
- [10] D. Turnbull, *Contemp. Phys.* **1969**, 10, 473.

- [11] S. Wei, Z. Evenson, M. Stolpe, P. Lucas, C. A. Angell, *Sci. Adv.* **2018**, 4, eaat8632.
- [12] S. Wei, C. Persch, M. Stolpe, Z. Evenson, G. Coleman, P. Lucas, M. Wuttig, *Acta Mater.* **2020**, 195, 491.
- [13] J. C. Mauro, Y. Yue, A. J. Ellison, P. K. Gupta, D. C. Allan, *Proc. Natl. Acad. Sci. USA* **2009**, 106, 19780.
- [14] C. A. Angell, *Science* **1995**, 267, 1924.
- [15] S. Wei, P. Lucas, C. A. Angell, *MRS Bull.* **2019**, 44, 691.
- [16] M. Chen, K. A. Rubin, *Proc. SPIE* **1989**, 1078, 150.
- [17] Y. M. Chen, G. X. Wang, L. J. Song, X. Shen, J. Q. Wang, J. T. Huo, R. P. Wang, T. F. Xu, S. X. Dai, Q. H. Nie, *Cryst. Growth Des.* **2017**, 17, 3687.
- [18] B. Chen, D. de Wal, G. H. ten Brink, G. Palasantzas, B. J. Kooi, *Cryst. Growth Des.* **2018**, 18, 1041.
- [19] M. H. R. Lankhorst, *J. Non-Cryst. Solids* **2002**, 297, 210.
- [20] M. K. Santala, B. W. Reed, S. Raoux, T. Topuria, T. LaGrange, G. H. Campbell, *Appl. Phys. Lett.* **2013**, 102, 174105.
- [21] Y. Chen, S. Mu, G. Wang, X. Shen, J. Wang, S. Dai, T. Xu, Q. Nie, R. Wang, *Appl. Phys. Express* **2017**, 10, 105601.
- [22] J. Pries, S. Wei, M. Wuttig, P. Lucas, *Adv. Mater.* **2019**, 31, 1900784.
- [23] J. A. Kalb, M. Wuttig, F. Spaepen, *J. Mater. Res.* **2007**, 22, 748.
- [24] J. Pries, S. Wei, F. Hoff, P. Lucas, M. Wuttig, *Scr. Mater.* **2020**, 178, 223.
- [25] Y. Z. Yue, S. L. Jensen, J. deC. Christiansen, *Appl. Phys. Lett.* **2002**, 81, 2983.
- [26] C. A. Angell, Y. Yuanzheng, W. Li-Min, R. D. C. John, B. Steve, M. Stefano, *J. Phys. Condens. Matter* **2003**, 15, S1051.
- [27] L. Hu, Y. Yue, *J. Phys. Chem. C* **2009**, 113, 15001.
- [28] G. W. Scherer, *Relaxation in Glass and Composites*, Wiley, New York **1986**.
- [29] S. Wei, P. Lucas, C. A. Angell, *J. Appl. Phys.* **2015**, 118, 034903.
- [30] A. Schlieper, Y. Feutelais, S. G. Fries, B. Legendre, R. Blachnik, *Calphad* **1999**, 23, 1.
- [31] R. Sengottaiyan, N. Saxena, K. D. Shukla, A. Manivannan, *J. Phys. D Appl. Phys.* **2020**, 53, 025108.
- [32] C. Adenis, V. Langer, O. Lindqvist, *Acta Crystallogr., Sect. C: Struct. Chem.* **1989**, 45, 941.
- [33] P. Bauer Pereira, I. Sergueev, S. Gorsse, J. Dadda, E. Müller, R. P. Hermann, *Phys. Status Solidi B* **2013**, 250, 1300.